

December 2005

## Strong terahertz emission from (100) p-type InAs

Rajind Mendis

*University of Wollongong*, [rajind@uow.edu.au](mailto:rajind@uow.edu.au)

M. L. Smith

*University of Wollongong*

L. J. Bignell

*University of Wollongong*

R. Vickers

*University of Wollongong*, [rv@uow.edu.au](mailto:rv@uow.edu.au)

R. A. Lewis

*University of Wollongong*, [roger@uow.edu.au](mailto:roger@uow.edu.au)

Follow this and additional works at: <https://ro.uow.edu.au/engpapers>



Part of the [Engineering Commons](#)

<https://ro.uow.edu.au/engpapers/160>

---

### Recommended Citation

Mendis, Rajind; Smith, M. L.; Bignell, L. J.; Vickers, R.; and Lewis, R. A.: Strong terahertz emission from (100) p-type InAs 2005.

<https://ro.uow.edu.au/engpapers/160>

## Strong terahertz emission from (100) *p*-type InAs

R. Mendis, M. L. Smith, L. J. Bignell, R. E. M. Vickers, and R. A. Lewis

*Institute for Superconducting and Electronic Materials, University of Wollongong, Wollongong, New South Wales 2522, Australia*

(Received 6 January 2005; accepted 7 November 2005; published online 28 December 2005)

Terahertz emission has been observed from (100) Zn-acceptor-doped InAs under illumination by fs pulses of near-infrared radiation. Turning the crystal about the surface normal produces two maxima per rotation, whether the angle of incidence is 45° or 75°, in contrast to (111) *p*-InAs, where three maxima per rotation have been reported. The emitted terahertz power has a quadratic variation with the pump power and decreases with increasing temperature in the range 20–300 K. This behavior is consistent with a photocurrent surge being the dominant terahertz generating mechanism at low excitation fluences. The *p*-type InAs generates about two orders of magnitude more power than the standard unbiased terahertz emitter, 1 mm thick ZnTe. © 2005 American Institute of Physics.

[DOI: 10.1063/1.2149161]

Schemes for generating terahertz (THz) radiation have proliferated in recent years. Many of these are based on using ultrafast optical pulses to excite a suitable target.

Photoconductive (PC) antennas are often regarded as being the most efficient emitters but suffering from restricted bandwidth. Recently great gains have been made in increasing the emitted bandwidth. PC antennas based on multi-energy arsenic-ion-implanted GaAs and semi-insulating GaAs,<sup>1</sup> while broadband (to 30 THz), do not have as good signal-to-noise ratios as those based on L(ow)T(emperature)-GaAs, which also contain frequency components to 30 THz.<sup>2</sup> Asymmetric excitation and a backward collection scheme were employed to achieve this result.<sup>2</sup> The critical role of post-growth annealing has been identified.<sup>3</sup> Combined with LT-GaAs receivers, an all-PC system with frequency components up to 7.5 THz has been developed.<sup>4</sup> Apart from the material properties,<sup>5,6</sup> the output from PC antennas also depends critically on the design of the electrodes.<sup>7</sup> Further sophistication such as the incorporation of Bragg mirrors has been pursued.<sup>8</sup>

Of electro-optic (EO) emitters, ZnTe is the most widely employed. EO emitters require neither biasing nor cooling and so are much simpler to use than PC antennas. While the efficiency of EO emitters is less than that of PC emitters, in some cases the absolute power realized is greater. The bandwidth is often greater.

A third class of emitters is those that rely on the separation and acceleration of charges, giving rise to a surge current even in the absence of an applied bias. A surface electric field may be the cause of the charge separation; alternatively the differential diffusion of holes and electrons generated by illumination (the photo-Dember effect) may be responsible. Such emitters have the simplicity of operation of the EO emitters but the potential for the greater efficiency of the PC emitters. Systematic work on *n*-type (100) InAs<sup>9</sup> has revealed an optimum temperature, in the range 3–300 K, of 170 K and a power that increased with an applied magnetic field up to the highest field used, 8 T. Varying the temperature to optimize the THz output has also been effective in the

case of InSb,<sup>10,11</sup> presumed due to an increase in band bending as the temperature decreased.

Adomavičius *et al.*<sup>12</sup> have recently reported on the emission of THz radiation from *p*-InAs. They point out the critical importance of the polarity of the dopant, showing acceptor-doped InAs to be a far stronger emitter than donor-doped InAs. They explain their observations as being due to electrical-field-induced optical rectification in a large surface-depletion layer. The data they presented were concerned exclusively with (111) samples. Here we present experimental observations on (100) *p*-type InAs.

The samples studied were *p*-type Zn-doped InAs with front surface epi-ready polished and normal to (100)±0.1°. Carrier concentration at 77 K was specified by the manufacturer to be  $(0.93\text{--}2.1) \times 10^{16} \text{ cm}^{-3}$  and etch pit density to be  $(1.9\text{--}3.7) \times 10^4 \text{ cm}^{-2}$ .

We used room temperature THz reflection spectroscopy to independently determine an upper limit for the carrier concentration. For this we employed a Bomem DA3 Fourier-transform spectrometer furnished with a near-normal incidence stage and a DTGS detector. The result shown in Fig. 1 is a classic example of a polar material. The vertical lines indicate the energies of the transverse-optical (TO) and the longitudinal-optical (LO) phonons as given by Li *et al.*<sup>13</sup> as 217.3 cm<sup>-1</sup> and 238.5 cm<sup>-1</sup>, respectively. The horizontal lines indicate the reflectivity calculated from the refractive index. (The imaginary part *k* is taken to be 0.) The high-frequency refractive index is taken to be *n*=3.5 from Li *et al.*<sup>13</sup> the low-frequency refractive index is calculated to be 3.84 using the Lyddane–Sachs–Teller relation. The observed reflectivity spectrum is consistent with these indices. The main information we gain from these data is that the sample is lightly doped. There is no evidence of the plasma above 100 cm<sup>-1</sup>. Li *et al.*<sup>13</sup> give the plasma frequency as 107 cm<sup>-1</sup> for a sample of carrier concentration  $6 \times 10^{16} \text{ cm}^{-3}$ . We conclude that the doping of the sample studied here is less than that.

Through low-temperature (1.5 K) THz transmission measurements we have sought transitions from the ground state to the excited states of the Zn acceptor in this InAs

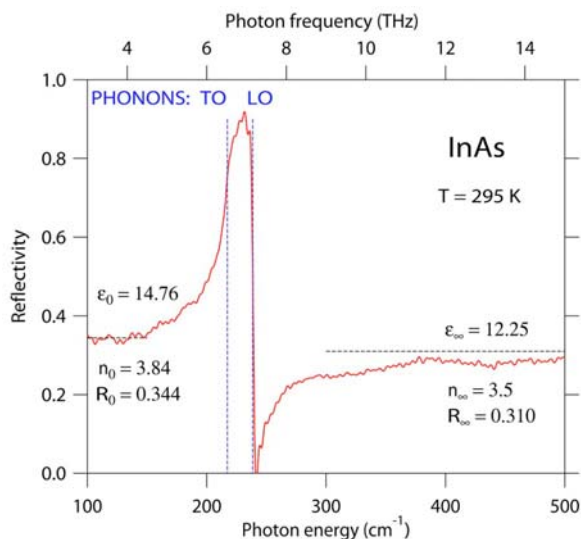


FIG. 1. (Color online) Room temperature reflection spectrum of *p*-InAs sample at near-normal incidence.

sample, as have been observed, for example, in Zn-doped InP.<sup>14</sup> We closely examined the region below 3 THz, presuming the ionization energy to be  $E_A \sim 0.01$  meV. So far we have not been able to detect these transitions, probably because of wave function overlap. The impurity lines become broadened beyond recognition at comparable concentrations in cognate systems, such as for the Be acceptor in GaAs.<sup>15</sup>

In the succeeding experiments, the InAs crystal was illuminated by ultrashort pulses of center wavelength 790 nm produced by a Femtosource Compact Pro 12 fs oscillator.<sup>16</sup> The beam was incident at either 45° or 75° (the Brewster angle) and focused onto the sample by an  $f=10$  cm lens. The THz radiation was detected at the specular reflection angle by He-cooled 4.2 K or 1.5 K Si bolometers, after passing through a polystyrene sheet, a Si plate, and a cold 3 THz cutoff filter. The polystyrene and Si were crucial in minimizing the background signal on the bolometer. Lock-in detection was used with a 300 ms time constant, chopping at 183 Hz.

The sample was rotated by azimuthal angle  $\theta$  about the surface normal for angles of incidence 45° and 75°. The dependence of the THz power on  $\theta$  is shown in Fig. 2. In this figure, the power has been normalized to an average power of 1. The same dependence on  $\theta$  of the generated THz power is observed for the two angles of incidence. The dependence follows a  $\cos 2\theta$  behavior superimposed on a substantial background. This suggests a dominant photocurrent surge (associated with the large constant background) and a minor optical rectification process (associated with the small angular dependence) contributing to the production of the THz radiation. As expected from the equations governing the optical rectification,<sup>17</sup> the  $\cos 2\theta$  dependence is consistent with optical rectification for (100) orientation, just as a  $\cos 3\theta$  dependence has been noted for (111) orientation.<sup>12</sup> A  $\cos 2\theta$  dependence has been observed previously for (100) orientation in, for example, *n*-type InAs (Ref. 18) and *n*-type InSb.<sup>17</sup> The combined data in Fig. 2 has been fitted with the function  $f(\theta) = 1 + \alpha \cos 2\theta$  and it is found that  $\alpha$

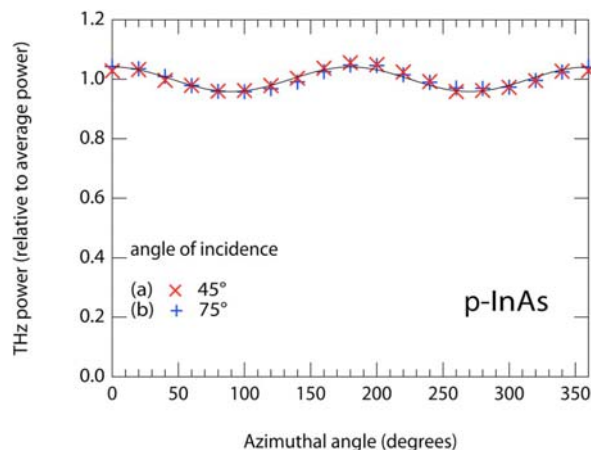


FIG. 2. (Color online) Dependence of THz power on azimuthal angle for angles of incidence (a) 45° and (b) 75°. The full line is the fit  $f(\theta) = 1 + \alpha \cos 2\theta$  with  $\alpha = 0.041$ .

$= 0.041 \pm 0.002$ . This fit is displayed as the full line in the figure.

The dependence of the THz power on the power of the pump laser has been measured. To facilitate a comparison with other work, where the THz electric field amplitude is given as a function of pump power, the square root of the THz power is plotted against pump power in Fig. 3. The data for the two incidence angles are shown normalized to 1 for the maximum pump power (228 mW). The full line shown in Fig. 3 joins (0,0) and (228 mW, 1). It is seen that the variation of THz power with pump power is close to quadratic. The data in Fig. 3 are for an azimuthal angle  $\theta = 0^\circ$ . We have also measured at an azimuthal angle  $\theta = 90^\circ$ , and observed a similar behavior. In comparison to pump power/fluence dependencies of THz signals given earlier,<sup>12,18</sup> our measurements are at much lower pump fluences ( $< 1 \mu\text{J}/\text{cm}^2$ ) and are characteristic of a photocurrent surge mechanism, more specifically the photo-Dember effect as re-

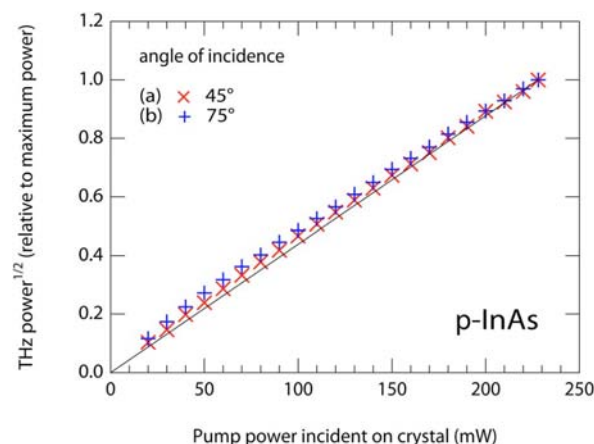


FIG. 3. (Color online) Variation of  $(\text{THz power})^{1/2}$  on near-infrared fs pump power for angles of incidence (a) 45° and (b) 75°. The  $1/e^2$  intensity diameter of the pump beam is approximately 0.75 mm. This is equivalent to an excitation fluence (or energy density) normal to beam propagation of approximately  $1 \mu\text{J}/\text{cm}^2$  at 250 mW pump power. The dependence of the output power on the input power is close to quadratic.

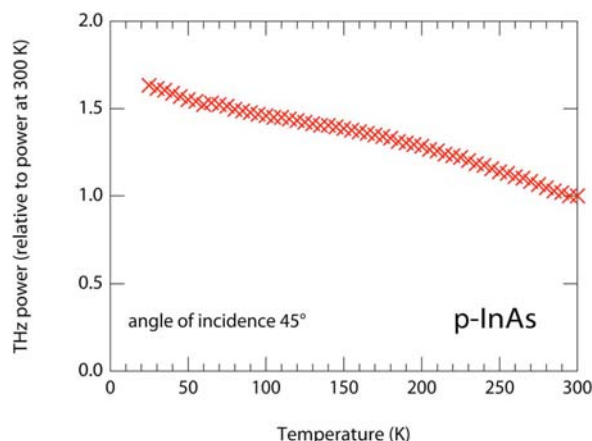


FIG. 4. (Color online) Variation of THz power with temperature for angle of incidence  $45^\circ$ .

ported previously for THz generation under low excitation fluences.<sup>17,19</sup> As the radiating dipole due to the current surge is oriented perpendicular to the surface, the emitted THz radiation would be *p* polarized. The small angular dependence on crystallographic orientation seen in Fig. 2 is possibly due to a minor contribution from bulk optical rectification, although it is not possible to completely rule out other nonlinear processes—such as electric-field-induced optical rectification or surface nonlinear optical response—without further experimental evidence.<sup>12,18</sup>

The dependence of the THz power on the temperature has been measured over the range 20–300 K. The results are shown in Fig. 4, normalized to a power of 1 at 300 K. In contrast to undoped, residual *n*-type (100) InAs, for which a maximum in power is observed at  $\sim 170$  K,<sup>9</sup> but in agreement with data for undoped (111) InSb,<sup>10,11</sup> our data show a steady decrease in power with temperature. Cooling improves the emitter performance at a rate of approximately 1% per 5 K. We attribute the increase in THz power at low temperature to an increase in carrier mobility, consistent with the proposed dominant carrier transport mechanism.

We have compared the THz power generated from *p*-InAs with that generated from ZnTe under similar conditions. While we used exactly the same pump laser and delivery optics and the same THz filters and detector, it is not possible to compare the two emitters exactly as one is used in a transmission geometry and the other in reflection. We chose the best orientation for the ZnTe emitter regarding incidence angle, in this case near-normal, and the best azimuthal angle to maximize the signal; likewise for the InAs emitter we chose the best incidence angle, in this case the Brewster angle, and the best azimuthal angle to maximize the signal. We note an advantage of using the *p*-InAs at the Brewster angle over the ZnTe is that the geometry eliminates

TABLE I. Comparison of THz power generated by 1 mm thick ZnTe and *p*-type InAs under similar conditions of excitation and detection.  $\theta_i$  is the angle of incidence.

ZnTe	Transmission	1
<i>p</i> -InAs	$\theta_i = 45^\circ$	54
<i>p</i> -InAs	$\theta_i = 75^\circ$	88

the near-infrared beam from the emitted THz beam removing the necessity for further filtering. We chose the best of four ZnTe crystals of different thicknesses and from two different suppliers to compare with the *p*-InAs. The results are given in Table I. The *p*-InAs emitter generates about two orders of magnitude more THz power than the standard 1 mm thick ZnTe emitter. Our preliminary estimate is an average THz power of about 100 nW at the highest pump power.

## ACKNOWLEDGMENT

This work was supported by the Australian Research Council. We acknowledge the support of Professor Chao Zhang.

- <sup>1</sup>T.-A. Liu, M. Tani, M. Nakajima, M. Hangyo, and C.-L. Pan, Appl. Phys. Lett. **83**, 1322 (2003).
- <sup>2</sup>Y. C. Shen, P. C. Upadhyay, E. H. Linfield, H. E. Beere, and A. G. Davies, Appl. Phys. Lett. **83**, 3117 (2003).
- <sup>3</sup>I. S. Gregory, C. Baker, W. R. Tribe, M. J. Evans, H. E. Beere, E. H. Linfield, A. G. Davies, and M. Missous, Appl. Phys. Lett. **83**, 4199 (2003).
- <sup>4</sup>Y. C. Shen, P. C. Upadhyay, H. E. Beere, E. H. Linfield, A. G. Davies, I. S. Gregory, C. Baker, W. R. Tribe, and M. J. Evans, Appl. Phys. Lett. **85**, 164 (2004).
- <sup>5</sup>R. Yano, H. Gotoh, Y. Hirayama, and S. Miyashita, J. Appl. Phys. **96**, 3635 (2004).
- <sup>6</sup>J. Zhang, Y. Hong, S. L. Braunstein, and K. A. Shore, IEEE Proc.: Optoelectron. **151**, 98 (2004).
- <sup>7</sup>M. R. Stone, M. Naftaly, R. E. Miles, J. T. Fletcher, and D. P. Steenson, IEEE Trans. Microwave Theory Tech. **52**, 2420 (2004).
- <sup>8</sup>J. Darmo, T. Muller, G. Strasser, K. Unterrainer, and G. Tempea, Electron. Lett. **39**, 460 (2003).
- <sup>9</sup>R. McLaughlin, Q. Chen, A. Corchia, C. M. Cielsa, D. D. Arnone, X.-C. Zhang, G. A. C. Jones, E. H. Linfield, and M. Pepper, J. Mod. Opt. **47**, 1847 (2000).
- <sup>10</sup>S. C. Howells, S. D. Herrera, and L. A. Schlie, Appl. Phys. Lett. **65**, 2946 (1994).
- <sup>11</sup>S. C. Howells and L. A. Schlie, Appl. Phys. Lett. **67**, 3688 (1995).
- <sup>12</sup>R. Adomavičius, A. Urbanowicz, G. Molis, A. Krotkus, and E. Šatkovskis, Appl. Phys. Lett. **85**, 2463 (2004).
- <sup>13</sup>Y. B. Li, R. A. Stradling, T. Knight, J. R. Birch, R. H. Thomas, C. C. Phillips, and I. T. Ferguson, Semicond. Sci. Technol. **8**, 101 (1993).
- <sup>14</sup>R. A. Lewis and Y.-J. Wang, Solid State Commun. **126**, 275 (2003).
- <sup>15</sup>R. A. Lewis, T. S. Cheng, M. Henini, and J. M. Chamberlain, Phys. Rev. B **53**, 12829 (1996).
- <sup>16</sup>See [www.femtolasers.com](http://www.femtolasers.com)
- <sup>17</sup>P. Gu, M. Tani, S. Kono, K. Sakai, and X.-C. Zhang, J. Appl. Phys. **91**, 5533 (2002).
- <sup>18</sup>M. Reid and R. Fedosejevs, Appl. Phys. Lett. **86**, 011906 (2005).
- <sup>19</sup>H. Takahashi, A. Quema, M. Goto, S. Ono, and N. Sarukura, Jpn. J. Appl. Phys., Part 2 **42**, L1259 (2003).